CrystEngComm

PAPER

View Article Online
View Journal | View Issue

Cite this: *CrystEngComm*, 2018, **20**, 1383

L-Malic acid crystallization: polymorphism, semi-spherulites, twisting, and polarity†

Jingxiang Yang,[ab] Chunhua T. Hu,[a] Alexander G. Shtukenberg,[a] Qiuxiang Yin*[b] and Bart Kahr*[ac]

Received 6th December 2017,
Accepted 17th January 2018

DOI: 10.1039/c7ce02107k

rsc.li/crystengcomm

L-Malic acid (LMA) is a commodity chemical that was first isolated in the crystalline form in the 18th century, yet it has been troublesome for more than 100 years because of its resistance to forming crystals that are suitable for optical or X-ray analysis. LMA crystallizations from the melt and from solutions are reevaluated here. Indeed, LMA crystallizes poorly from water. However, a flowable solid was produced by growth from ethyl acetate at room temperature to give large well-formed trapezoidal prisms of a new LMA polymorph, form II (space group $P2_1$, a = 5.7343(6) Å, b = 6.7990(7) Å, c = 6.9949(7) Å, β = 104.9610(10)°, V = 263.47(5) Å^3, Z = 2). The growth of LMA from ethyl acetate at 4 °C produced hard, near-spherical aggregates of the only previously known phase, which also crystallizes in the space group $P2_1$ (form I). From the melt, LMA produces spherulites with helicoidal twisting of its individual fibrils. Polycrystalline ensembles are shown to arise from the inequivalent branching of the ends of a polar crystal which adopt semi-spherulitic morphologies as crystallization intermediates. Tailor-made additives were used to assign the absolute growth direction of the polar spherulite radii as +b.

Introduction

L-(−)-Malic acid (LMA), isolated by Scheele from apple juice in 1785,[1,2] is a major food additive (US production, *ca.* 5000 tons per annum), but the formation of sizable, well-formed LMA crystals has been a long-standing challenge. Groth reported that LMA crystallizes from water "with difficulty in the form of deliquescent needles that serve no useful purpose".[3] By this, he probably meant that they could not be indexed. In fact, when grown from water in our hands, the crystals are small, irregular, and platy (Fig. 1). Little improvement can be achieved with acetone, ethanol, acetonitrile, isopropanol, 1-propanol and 1-butanol solvents. The ill-defined morphologies do not lead to easily-described habits. An X-ray structure of this form was not reported until 1989 by authors quoting Groth's lament to emphasize their technical challenges, albeit they did succeed with water as the solvent. Crystal data: space group $P2_1$, a = 5.041(1) Å, b = 9.188(3) Å, c = 11.792(4) Å, β = 94.06(2)°, V = 544.8(3) Å^3, Z' = 2, Z = 4.[4]

Small crystals with high-aspect-ratio habits frequently raise difficulties in downstream processing operations, such as filtration, storage, packing, and tablet-making or capsule-filling.[5–7] Larger particles with high sphericity are superior for filterability, flowability, compactibility, and bulk density.[8–15] Many problems can be solved by the unit operation or granulation *via* adhesion of smaller particles following crystallization.[16] Alternatively, the so-called spherical crystallization, *i.e.* direct agglomeration of crystallites with the

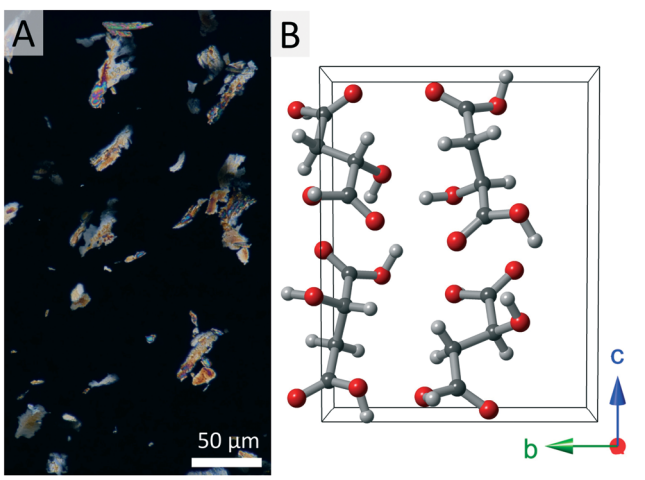

Fig. 1 (A) Poorly formed L-malic acid form I crystals grown from aqueous solution observed between crossed polarizers and (B) its crystal structure[4] viewed along the *a* axis.

[a] *Department of Chemistry and Molecular Design Institute, New York University, 100 Washington Square East, Room 1001, New York City, NY 10003, USA. E-mail: bart.kahr@nyu.edu*
[b] *School of Chemical Engineering and Technology, Tianjin University, Tianjin 300072, P. R. China*
[c] *Department of Advanced Science and Engineering (TWins), Waseda University, 162-0056, Tokyo, Japan*

† CCDC1 1586384. For crystallographic data in CIF or other electronic format see DOI: 10.1039/c7ce02107k

addition of partially miscible liquids during the original precipitation process, can likewise improve the flowability.[17,18] But the addition of binders in this process requires recycling and separation of the organic solvents. It would be much more efficient to grow large crystals with a smaller aspect-ratio, obviating the need for fillers or binders.

In this paper, we improve the flowability of poorly crystallizing LMA without additives in two ways: (1) by crystallizing to a new polymorph; and (2) by inducing spherulitic crystallization. We also show how to control the size of spherulites using tailor-made additives, which, moreover, is a method for assigning the absolute crystallographic orientation of spherulitic fibers growing along a polar axis. Additionally, we report that under some conditions, the individual crystallites in spherulites are twisted, a phenomenon now observed so frequently it can no longer be considered unusual.

Results and discussion

Polymorphism

We confirmed that LMA does indeed crystallize with difficulty from water (under vacuum of 9.5 kPa at 20 °C), producing irregular, platy particles that best resemble birefringent "smudges" (for the lack of a more crystallographically precise description) on a dark field, as shown in Fig. 1a. These were identified by Raman microscopy and powder X-ray diffraction as form I whose crystal structure is shown in Fig. 1b.[4]

In contrast to the difficulties observed in crystallizing LMA from water, ethyl acetate solutions at 20–21 °C precipitate large well-formed trapezoidal prisms (Fig. 2a). Singe crystal X-ray diffraction analysis reveals that these crystals are a new polymorph, form II, also crystallizing in the space group $P2_1$ but with $Z' = 1$ rather than $Z' = 2$ as in form I. Crystal data: a = 5.7343(6), b = 6.7990(7), c = 6.9949(7) Å, β = 104.961(1)°, V = 263.47(5) Å^3 (Fig. 2b). The trapezoids are shaped by {011}, {0$\bar{1}\bar{1}$}, {2$\bar{1}\bar{1}$}, and {101} facets. The absolute polar direction of the crystal was not established by X-ray analysis because the anomalous dispersion was small.

Single crystals of form II are large (0.1 mm^3) and polyhedral. As shown by differential scanning calorimetry, form II transforms into form I at 89 °C (scan rate of 10° min^{-1}) with a phase transition enthalpy of 5.36 kJ mol^{-1}. The transformation begins on crystal surfaces at lower temperature (60 °C), as evidenced by hot stage polarized light optical microscopy. The crystals became opaque but preserved their polyhedral envelopes. Therefore, after transformation, the stable form I crystals have the same particle sizes and shapes inherited from the more flowable form II.

Spherulites

Growing polyhedral single crystals of form II is not the only strategy we found to improve the powder performance of LMA without the aid of additives. Crystallization from ethyl acetate at 4–5 °C produced nearly spherical aggregates, as shown in Fig. 3. These particles were confirmed to be form I by Raman microscopy and X-ray powder diffraction. Compared to the small, platy microcrystals (20 μm) grown from water, the spherulitic particles are much larger (around 800 μm) and spherical. Observations with a polarized light optical microscope established the spherulitic structure of these particles (Fig. 3 inset).

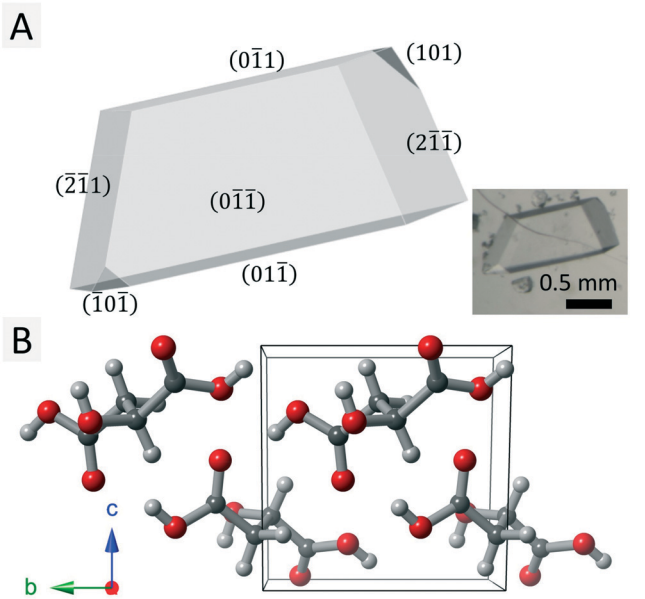

Fig. 2 (A) Morphology of L-malic acid form II created using WinXMorph™.[19,20] The inset is a micrograph of a single crystal. (B) The crystal structure of form II viewed along the *a* axis.

The flowability of three different products was characterized with the Carr index[5] (Table 1). The Carr indices of both polyhedral crystals and spherulitic particles are much lower than those of the fine powder of form I, as purchased from Sigma-Aldrich, with irregularly shaped particles. Large polyhedral crystals and spherulites with aspect ratios close to one

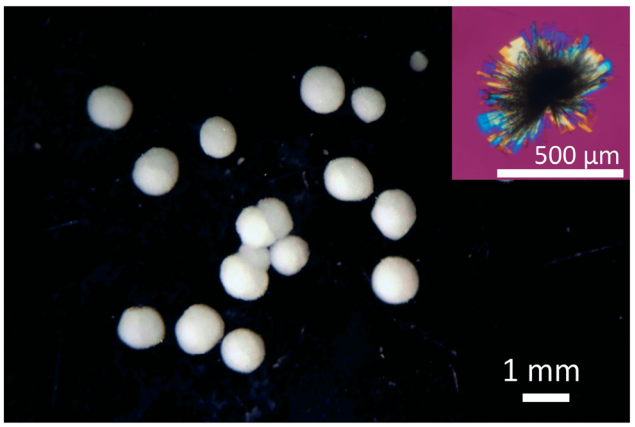

Fig. 3 Spherulitic particles of L-malic acid grown in ethyl acetate solution. The inset shows the radial arrangement of crystallites between crossed polarizers with a first order red retarder. The spherulites have positive birefringence, indicating that the slow axis or larger refractive index is radial rather than tangential.

Table 1 Characterization of the physicochemical properties of LMA products

Morphology	Polymorph	Bulk density (g mL^{-1})	Tapped[d] density (g mL^{-1})	Carr[e] index
Irregular powder[a]	Form I	0.666	0.913	0.270
Polyhedral crystals[b]	Form II	0.673	0.707	0.048
Spherulitic particles[c]	Form I	0.661	0.697	0.053

[a] Purchased from Sigma-Aldrich Co. LLC. [b] Grown from ethyl acetate solutions at 20–21 °C. [c] Grown from ethyl acetate solutions at 4–5 °C. [d] Obtained by tapping the powder in a graduated cylinder until no more volume change is observed. [e] See text.

flow more easily than smaller crystallites with a dispersion of shapes.

Spherulites are generally regarded as a source of trouble. The term "spherulite" is sometimes used pejoratively, and even incorrectly, to describe a failed attempt to prepare well-defined single crystals. Recently, spherulitic growth has become recognized as a practical outcome. Spherulites of microbial polyhydroxyalkanoates and amylose inclusion complexes were evaluated as drug delivery vehicles while spherulites of human interferon had improved pharmacokinetics.[21–23] Spherulitic growth can also be used in product design. For example, the formation of spherulitic particles was used to increase the filterability of $CaCO_3$ crystals.[24] L-Tryptophan particles with better flowability and higher bulk density were prepared *via* polymer-induced spherulitic growth.[25] In addition to improving the LMA powder performance by growing large, compact spherulites, there remained features of LMA crystallization that warranted further analysis such as morphology evolution and microstructure.

Twisting

We were aware of early reports that LMA grows from the melt as optically banded spherulites[26–28] in which rhythmic optical properties are characteristic of helicoidal twisting of fibrils growing radially.[29–33] The helicoidal twisting of molecular crystals as they grow was a lost aspect of organic crystallography.[11,34–36] We have recently studied this phenomenon in a variety of other molecular crystals.[37–44] We observed optically banded spherulites of LMA when it was crystallized from the melt (Fig. 4A–D). Scanning electron micrographs show that the optical bands corresponded to crystallites alternately growing in edge-on and face-on orientations, smoothly rotating from one orientation to the other with the sense of left-handed helicoids. Naturally, D-malic acid produces right-handed helicoids. This was confirmed by Wallerant's method of "sensing the screw",[26–28,35–37,45,46] watching the extinction bands move up or down like a barber-shop striped pole as the spherulite is rotated around a radial axis.

Absolute polarity

X-ray diffraction texture analysis on the spherulitic film indicated that the spherulites were growing along the *b* axis, a polar axis in the space group $P2_1$. Spherulites typically grow by small angle branching of unstable ends of a single crystal nucleus. However, if the ends of a needle-shaped nucleus correspond to those of a polar axis, a spherical shape may not develop quickly, especially if growth and branching along the $+b$ and $-b$ directions occurs at different rates. The left side of the crystalline aggregate in Fig. 4A shows the typical optical texture of a banded spherulite made from twisted fibrils; however, the right side shows the fanning of untwisted crystallites, without rhythmic optical properties. These objects might be more properly described as semi-spherulites, or hemi-spherulites, were they not pressed between glass slides and free to grow in a third direction. The fans were

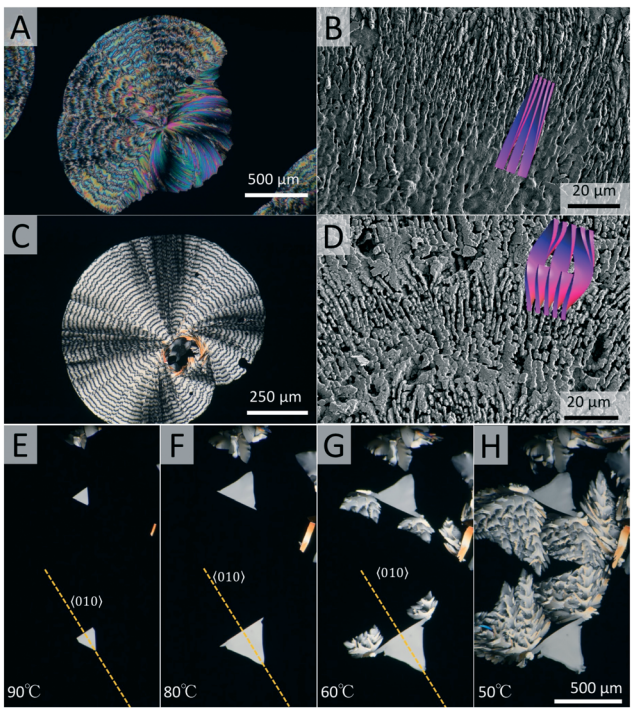

Fig. 4 L-Malic acid crystallizing from the melt. (A and B) Banded spherulites of L-malic acid: (A) periodic extinction pattern observed between crossed polarizers; (B) SEM image of twisted fibers, and schematic forms as purple overlays. (C and D) Banded spherulites of L-malic acid grown in the presence of 15 wt% L-threitol (50 °C): (C) view between crossed polarizers; (D) corresponding SEM image with a scheme highlighting the twist; the gaps between different parts of individual lamellae are likely to be a result of thermal stress during sample quenching, mechanical damage during sample preparation, or partial L-malic acid sublimation under high vacuum conditions. (E–H) Transformation from a single crystal into a semi-spherulitic shape by decreasing the crystallization temperature. The yellow dotted line shown in (E–G) is the diad axis.

suppressed with the addition of 15 wt% L-threitol to the melt (Fig. 4C). In this way, the semi-spherulites will ultimately close to form a circumference with twisted crystallites growing in all radial directions, but all such branches originated from only one side of the initial nucleus. Rather than forming a pair of "eyes" near the nucleus,[47] voids encircled by small angle branching of crystallites from both sides of the initial "sheaf of wheat" morphology, LMA produces a "cyclops", a spherulite with just one eye.

The polarity of crystal growth can be clearly seen at low undercoolings, when the branching intensity is still low. At an undercooling of 10 °C, LMA forms crystals with equilateral triangular profiles. These are form I {001} crystals (Fig. 4E), as determined by powder X-ray diffraction. At larger undercoolings of 20 °C (Fig. 4A), small "feet" emerged on only one of the three sides. These features become unstable at undercoolings of 40 °C (Fig. 4G). Only in this way does small angle branching and spherulitic growth commence. However, the face normal to this direction remains stable despite the growth that then engulfs it (Fig. 4H). This transition from single crystal to polycrystalline growth establishes which direction is the singular diad axis in the triangular plates (the yellow dotted line in Fig. 4E–G).

These observations suggest that there might be two types of spherulites, depending on the polar direction. At first blush, these objects should look identical in a polarized light microscope, as radial aggregates of anisotropic lamellae or needles, quartered by dark extinction brushes. But depending upon which end of the polar axis grows more rapidly, there are two possible spherulitic formations shown schematically in Fig. 5. The positive directions of the radial polar axes might be pointing inward or outward, as indicated by the directions of the arrows. This is a kind of in–out diastereomorphism of polycrystalline ensembles that are not related by symmetry. Shimon *et al.* have shown that the fast direction of growth in polar single crystals of D, L-alanine can be switched by changing the solvent.[48] Thus, there is every reason to expect the possibility of polymorphous polycrystalline forms of the kind schematically illustrated in Fig. 5.

To assign the spherulite growth direction as [010] or [0$\bar{1}$0], we monitored the growth in the presence of tailor-made additives.[49–51] We previously established the absolute growth direction of β-resorcinol spherulites with polar radii in this way.[52] D-Tartaric acid and *meso*-tartaric acid were chosen to influence the habit of LMA spherulites. They can be recognized as hydroxy-substituted derivatives of LMA (Scheme 1). We anticipate that D-tartaric acid would selectively bind in the +*b* direction of form I, whereas *meso*-tartaric acid will bind in the −*b* direction (Fig. 6). In turn, these additives inhibit the growth of LMA along the +*b* and −*b* directions, respectively.

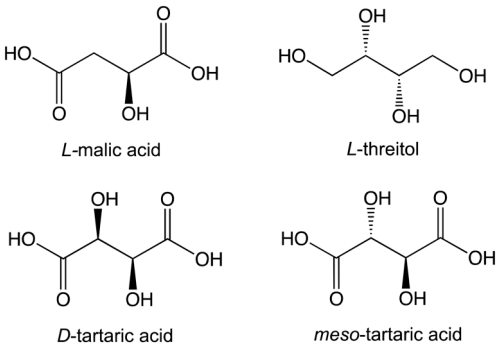

Scheme 1 Chemical structures discussed.

To strengthen our interpretation, we evaluated the growth of LMA spherulites in ethyl acetate with the addition of 1 wt% D-tartaric acid and *meso*-tartaric acid at 10 °C. (While threitol produced meaningful changes in the morphology of melt grown crystals, it did not influence the growth from solution). In the presence of 1 wt% *meso*-tartaric acid, LMA spherulites with the same size grew, as in the control experiment without the additive (Fig. 7). However, in the presence of 1 wt% D-tartaric acid, much smaller spherulites, only *ca.* 1% of the volume of those grown without additive, were deposited. Assuming that D-tartaric acid can adsorb more easily and inhibit +*b* growth as opposed to −*b* growth (Fig. 6), small spherulites with D-tartaric acid confirm radial +*b* growth. Thus, not only single crystals but also polycrystalline ensembles can be controlled with tailor-made additives.

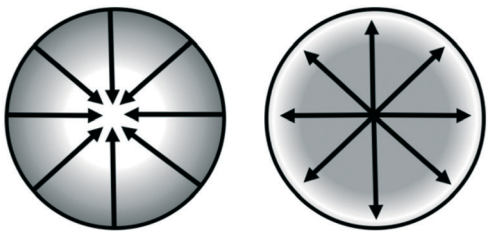

Fig. 5 Schematic illustration of the in–out "isomerism" of spherulites, for which the radial direction is a polar crystallographic axis indicated by arrows.

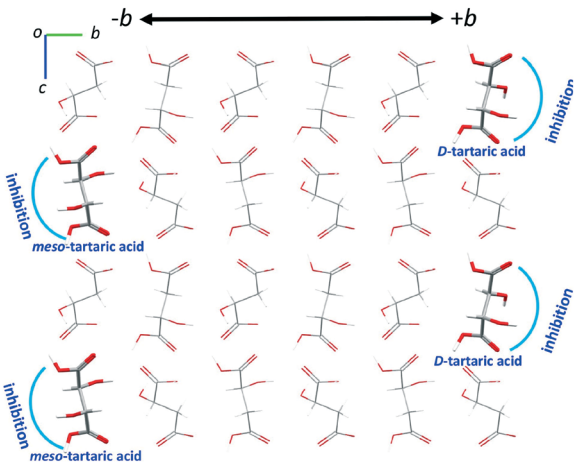

Fig. 6 (100) projection of the crystal structure of LMA form I. D-Tartaric acid and *meso*-tartaric acid bind selectively to the (010) and (0$\bar{1}$0) surfaces, respectively. Note that form I has $Z' = 2$.

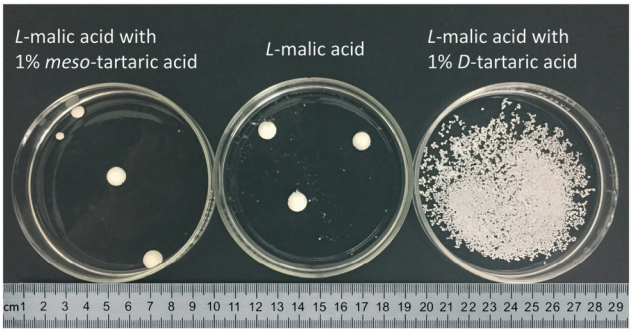

Fig. 7 The effect of tailor-made additives *meso*-tartaric acid (left) and D-tartaric acid (right) on the particle size of L-malic acid spherulites (grown at 10 °C from solutions saturated at 65 °C). The control experiment without the additive was depicted in the middle. The scale is expressed in cm.

Conclusion

In industry, controlling the particle size of crystalline materials is often a prerequisite to processing solids. We have discovered two effective ways to obtain particles of LMA, a widely-used food additive, with controlled sizes and better flowability than the product that is typically crystallized from water. First, a new polymorph of LMA was discovered as large trapezoidal prismatic crystals. Second, large, compact LMA spherulites were grown. By studying the microstructure and growth of spherulites with tailor-made additives, we assigned the absolute direction of the polar radial axis. This experiment not only identifies the absolute growth direction of LMA fibers in spherulites, but is also an example of the use of tailor-made additives to control the size of spherulitic particles. Twisted crystals were also grown from the melt but the mechanism that induces helicoidal morphologies in this instance remains unknown.

Experimental

Materials

L-Malic acid ($C_4H_6O_5$), D-malic acid ($C_4H_6O_5$), L-threitol ($C_4H_{10}O_4$), D-tartaric acid ($C_4H_6O_6$), *meso*-tartaric acid ($C_4H_6O_6$) and ethyl acetate were purchased from Sigma-Aldrich Co. LLC. Distilled, deionized water was used wherever applicable.

Crystallization

Single LMA (97%) crystals were grown by cooling to 20 °C a saturated ethyl acetate solution at 65 °C in a Pyrex crystallizing dish. Crystals from the melt were grown from a few mg of LMA placed between a microscope slide and a glass cover slip on a Kofler bench at *ca.* 120 °C. Some samples were remelted and subsequently crystallized on a hot stage (Model FP90, Mettler-Toledo). Polarized light micrographs were obtained with an Olympus BX50 microscope equipped with a digital camera.

Bulk properties

Both bulk density and tapped density of all products were determined using a measuring cylinder (25 mL). The Carr index was determined to evaluate the flowability of the powder.[5]

$$\text{Carr index} = \frac{\text{Tapped density} - \text{Bulk density}}{\text{Tapped density}}$$

X-ray diffraction

XRD patterns were collected on a Bruker AXS D8 DISCOVER GADDS microdiffractometer equipped with a VÅNTEC-2000 area detector, a sealed Cu tube, a graphite monochromator, and a 0.5 mm MONOCAP collimator (Cu Kα radiation, λ = 1.5418 Å). The data collection was performed in reflection mode either from as-grown crystalline films on a glass slide with the cover glass removed or from powder detached from the glass slide and attached to a silicon wafer with a small amount of vacuum grease.

Single-crystal structure determination

The X-ray intensity data of LMA form II was recorded on a Bruker D8 APEXII CCD system equipped with a sealed Mo X-ray tube, a graphite monochromator, and a 0.5 mm Mono-Cap collimator (Mo-Kα radiation, λ = 0.71073 Å). The crystal temperature was controlled at 100K using an Oxford Cryosystems 700+ cooler. Four sets of ω scans at four ϕ angles were collected. The 1600 frames acquired were processed with the INTEGRATE program of the APEX2 software for reduction and cell refinement. Multi-scan absorption corrections were applied by the SCALE program for the area detector. The structure of form II was solved by intrinsic phasing methods (SHELXT) and the structure models were completed and refined by full-matrix least-squares methods on F^2 (SHELXL). Non-hydrogen atoms in the structures were refined with anisotropic displacement parameters. Hydrogen atoms on carbons were placed in idealized positions (C–H = 0.95–1.00 Å) and included as riding with the heavy atoms (U_{iso}(H) = 1.2). Hydrogen atoms on oxygens were found from difference Fourier maps and refined with a restrained O–H distance of 0.84 Å. The crystallographic information file (CIF) including the HKL and RES data are deposited in the CCDC with no. 1586384.

Calorimetry

Differential scanning calorimetry (DSC) experiments were performed on a Perkin-Elmer DSC 8000 instrument with a scan rate of 10 °C min^{-1} under a nitrogen gas flow of 20 mL min^{-1} purge. Samples weighing 3–5 mg were heated in sealed non-hermetic aluminum pans. Two-point calibration using indium and tin was carried out to assess the temperature axis and heat flow of the equipment.

Scanning electron microscopy

Samples were mounted on conductive carbon tape after removal of the top coverslip, adhered to aluminum holders, and then coated with 5 nm of gold from an evaporator. The images were recorded with a MERLIN field-emission scanning electron microscope (Carl Zeiss) using a standard Everhart–Thornley type detector at an accelerating voltage of 1–2 kV.

Raman spectroscopy

Raman spectra were collected with a Thermo Scientific DXR Raman microscope (laser wavelength 532 nm, laser power 2 mW).

Conflicts of interest

The author declares no conflicts of interest.

Acknowledgements

B. K. thanks the U.S. National Science Foundation (NSF) (DMR-1105000 and DMR-1608374) for support of this research. This work was supported partially by the MRSEC program of the NSF under Award Number DMR-1420073. The X-ray facility was supported partially by the NSF under Award Number CRIF/CHE-0840277.

Notes and references

1 C. W. Scheele, *Kongliga Svenska Vetenskaps Akademiens Handlingar*, 1785, vol. 6, pp. 17–27 (in Swedish); An English translation may be found in, *The Collected Papers of Carl Wilhelm Scheele*, ed. L. Dobbins, Bell and Sons, London, 1931, pp. 267–275.
2 W. B. Jensen, *J. Chem. Educ.*, 2007, **84**, 924.
3 P. Groth, *Chemische Krystallographie*, Engelmann, Leipzig, 1910, vol. 3, p. 290.
4 P. Van der Sluis and J. Kroon, *Acta Crystallogr., Sect. C: Cryst. Struct. Commun.*, 1989, **45**, 1406.
5 R. L. Carr, *Chem. Eng.*, 1965, **72**, 69.
6 R. L. Carr, *Chem. Eng.*, 1965, **72**, 163.
7 H. G. Brittain, S. J. Bogdanowich, D. E. Bugay, J. DeVincentis, G. Lewen and A. W. Newman, *Pharm. Res.*, 1991, **8**, 963.
8 A. Castellanos, *Adv. Phys.*, 2005, **54**, 263.
9 J. P. Latham, A. Munjiza and Y. Lu, *Powder Technol.*, 2002, **125**, 10.
10 N. Peronius and T. J. Sweeting, *Powder Technol.*, 1985, **42**, 113.
11 R. Zou and A. Yu, *Powder Technol.*, 1996, **88**, 71.
12 A. Yu, J. Bridgwater and A. Burbidge, *Powder Technol.*, 1997, **92**, 185.
13 H. White and S. Walton, *J. Am. Ceram. Soc.*, 1937, **20**, 155.
14 A. Yu, C. Feng, R. Zou and R. Yang, *Powder Technol.*, 2003, **130**, 70.
15 P. Carman, *Chem. Eng. Res. Des.*, 1997, **75**, S32.
16 D. M. Parikh, *Handbook of Pharmaceutical Granulation Technology*, CRC Press, Washington DC, 2016.
17 Y. Kawashima, M. Okumura and H. Takenaka, *Science*, 1982, **216**, 1127.
18 J. Thati and Å. C. Rasmuson, *Eur. J. Pharm. Sci.*, 2011, **42**, 365.
19 W. Kaminsky, *J. Appl. Crystallogr.*, 2005, **38**, 566.
20 W. Kaminsky, *J. Appl. Crystallogr.*, 2007, **40**, 382.
21 M. Artsis, A. Bonartsev, A. Iordanskii, G. Bonartseva and G. Zaikov, *Mol. Cryst. Liq. Cryst.*, 2010, **523**, 21.
22 U. V. L. Ma, J. D. Floros and G. R. Ziegler, *Carbohydr. Polym.*, 2011, **83**, 1869.
23 Y. Jiang, K. Shi, D. Xia, S. Wang, T. Song and F. Cui, *J. Pharm. Sci.*, 2011, **100**, 1913.
24 R. Beck and J. P. Andreassen, *AIChE J.*, 2012, **58**, 107.
25 J. Yang, Y. Wang, H. Hao, C. Xie, Y. Bao, Q. Yin, J. Gong, C. Jiang, B. Hou and Z. Wang, *Cryst. Growth Des.*, 2015, **15**, 5124.
26 F. Wallerant, *C. R. Hebd. Seances Acad. Sci.*, 1906, **143**, 555.
27 F. Wallerant, *C. R. Hebd. Seances Acad. Sci.*, 1906, **143**, 1169.
28 F. Wallerant, *Bull. Soc. Fr. Mineral.*, 1907, **30**, 43.
29 B. Kahr and A. G. Shtukenberg, *Isr. J. Chem.*, 2016, **56**, 1.
30 P. Gaubert, *C. R. Hebd. Seances Acad. Sci.*, 1911, **153**, 683.
31 P. Gaubert, *Bull. Soc. Fr. Mineral.*, 1913, **36**, 45.
32 P. Gaubert, *C. R. Hebd. Seances Acad. Sci.*, 1918, **167**, 368.
33 P. Gaubert, *Bull. Soc. Fr. Mineral.*, 1918, **41**, 198.
34 F. Bernauer, "*Gedrillte*" *Kristalle*, Gebrüder Borntraeger, Berlin, 1929.
35 A. Shtukenberg, E. Gunn, M. Gazzano, J. Freudenthal, E. Camp, R. Sours, E. Rosseeva and B. Kahr, *ChemPhysChem*, 2011, **12**, 1558.
36 A. G. Shtukenberg, Yu. O. Punin, A. Gujral and B. Kahr, *Angew. Chem., Int. Ed.*, 2014, **53**, 672.
37 A. G. Shtukenberg, J. Freudenthal and B. Kahr, *J. Am. Chem. Soc.*, 2010, **132**, 9341.
38 B. Kahr, A. Shtukenberg, E. Gunn, D. J. Carter and A. L. Rohl, *Cryst. Growth Des.*, 2011, **11**, 2070.
39 A. Shtukenberg, J. Freudenthal, E. Gunn, L. Yu and B. Kahr, *Cryst. Growth Des.*, 2011, **11**, 4458.
40 A. G. Shtukenberg, X. Cui, J. Freudenthal, E. Gunn, E. Camp and B. Kahr, *J. Am. Chem. Soc.*, 2012, **134**, 6354.
41 X. Cui, A. L. Rohl, A. Shtukenberg and B. Kahr, *J. Am. Chem. Soc.*, 2013, **135**, 3395.
42 X. Cui, A. Shtukenberg, J. Freudenthal, S. M. Nichols and B. Kahr, *J. Am. Chem. Soc.*, 2014, **136**, 5481.
43 X. Cui, S. M. Nichols, O. Arteaga, J. Freudenthal, F. Paula, A. G. Shtukenberg and B. Kahr, *J. Am. Chem. Soc.*, 2016, **138**, 12211.
44 J. Yang, C. T. Hu, X. Zhu, Q. Zhu, M. D. Ward and B. Kahr, *Angew. Chem.*, 2017, **129**, 10299.
45 H. D. Keith and F. J. Padden, *J. Polym. Sci.*, 1959, **39**, 123.
46 D. Maillard and R. E. Prud'homme, *Macromolecules*, 2006, **39**, 4272.
47 A. G. Shtukenberg, Y. O. Punin, E. Gunn and B. Kahr, *Chem. Rev.*, 2012, **112**, 1805.

48 L. Shimon, M. Vaida, L. Addadi, M. Lahav and L. Leiserowitz, *J. Am. Chem. Soc.*, 1990, **112**, 6215.
49 L. Addadi, Z. Berkovitch-Yellin, I. Weissbuch, J. van Mil, L. J. W. Shimon, M. Lahav and L. Leiserowitz, *Angew. Chem., Int. Ed. Engl.*, 1985, **24**, 466.
50 Z. Berkovitch-Yellin, J. van Mil, L. Addadi, M. Idelson, M. Lahav and L. Leiserowitz, *J. Am. Chem. Soc.*, 1985, **107**, 3111.
51 I. Weissbuch, R. Popovitz-Biro, M. Lahav and L. Leiserowitz, *Acta Crystallogr., Sect. B: Struct. Sci.*, 1995, **51**, 115.
52 Q. Zhu, A. G. Shtukenberg, D. J. Carter, T.-Q. Yu, J. Yang, M. Chen, P. Raiteri, A. R. Oganov, B. Pokroy, I. Polishchuk, P. J. Bygrave, G. M. Day, A. L. Rohl, M. E. Tuckerman and B. Kahr, *J. Am. Chem. Soc.*, 2016, **138**, 4881.